CFD simulation of cyclone separator used for circulating fluidized bed boiler

Simulación cfd de un ciclón separador utilizado para la caldera de lecho fluidizado circulante



Haixia Li1, Bingguang Gao2, Bin li1, Xue Bai1 and Heo Jungwon3

- ¹ School of Mechanical and Power Engineering, Henan Polytechnic University, Jiaozuo 454000, China. lihx@hpu.edu.cn
- ² School of Application Techniques, Henan Polytechnic University, Jiaozuo 454000, China
- ³ Department of Chemical Engineering, Gyeongsang National University, Jinju 660-701, South Korea

DOI: http://dx.doi.org/10.6036/7933 | Recibido: 15/12/2015 • Aceptado: 02/02/2016

RESUMEN

- El separador de ciclón juega un papel crítico en la separación de partículas sólidas de los líquidos en una caldera de lecho fluidificado circulante. El problema de la deformación del tubo de exhaustación se produce cuando se utiliza un ciclón separador en plantas de energía. Esta deformación tiene una relación directa con la distribución del campo de flujo en separadores de ciclón. En este documento, se estudia el campo de flujo para mejorar el funcionamiento y la eficacia del separador de ciclón, por medio de técnicas de dinámica de fluidos computacional. El modelo de las tensiones de Reynolds proporcionado por el software FLUENT se aplica para el estudio de la dinámica del flujo de un separador de ciclón a tamaño natural utilizado para un lecho fluidizado circulante. Se investiga computacionalmente el efecto de la profundidad de inserción del tubo de exhaustación en el campo de flujo y el rendimiento del separador de ciclón. Los resultados demuestran que la caída de presión del separador de ciclón obtenida a partir de la simulación numérica concuerda bien con la caída de presión medida en un experimento en la planta de energía. La profundidad del tubo de exhaustación tiene un efecto insignificante sobre la caída de presión y la velocidad de distribución. La caída de presión aumenta inicialmente con la profundidad de inserción del tubo de exhaustación y luego disminuye con la profundidad de inserción del tubo de exhaustación. El tubo de exahustación ejerce una gran presión cuando la longitud del tubo de exhaustación es demasiado corta o demasiado grande. El aumento de la profundidad de inserción del tubo de exhaustación puede reducir el número de partículas que escapan del ciclón y mejorar la eficacia de separación. Los resultados de la investigación en un separador de ciclón de tamaño natural son importantes en la comprensión del comportamiento de un separador de ciclón grande para calderas de lecho fluidificado circulante en plantas de energía.
- Palabras clave: Separador de ciclón, Reynolds Stress Model (RSM), Simulación numérica, Tubo de exhaustación.

ABSTRACT

A cyclone separator plays a critical role in separating solid particles from fluids in a circulating fluidized bed boiler. The problem of exhaust pipe deformation occurs during the application of the cyclone separator in power plants. This deformation has a direct relationship with the flow field distribution in cyclone separators. In this paper, the flow field is explored to improve the operation and efficiency of the cyclone separator by means of computational fluid dynamic techniques. The Reynolds stress model pro-

vided by FLUENT software is applied to study flow dynamics of a full-size cyclone separator used for a circulating fluidized bed. The effect of the insert depth of the exhaust pipe on the flow field and performance of cyclone separator is investigated computationally. Results demonstrate that the pressure drop of the cyclone separator obtained from the numerical simulation agrees well with the pressure drop measured in an experiment in a power plant. The exhaust pipe depth has an insignificant effect on the pressure drop and velocity distribution. The pressure drop initially increases with the inset depth of the exhaust pipe and then decreases with the insert depth of exhaust pipe. The exhaust pipe exerts a large pressure when the exhaust pipe length is too short or too large. Increasing the insert depth of exhaust pipe can reduce the number of particles that escape from the cyclone and improve separation efficiency. Investigation results of full-size cyclone separator are significant in understanding the behavior of the large cyclone separator for circulating fluidized bed boilers in power plants.

Keywords: cyclone separator, Reynolds stress model (RSM), numerical simulation, exhaust pipe.

1. INTRODUCTION

Gas cyclone separators are widely used in industries to separate dust from gas because of their geometrical simplicity and relatively economic power consumption [1]. Cyclones may also be adopted for use in extreme operating conditions, such as high temperature, high pressure, and corrosive gases. Cyclones have no moving parts, thereby making them relatively maintenance free. Therefore, cyclones have found a high number of applications in the field of air pollution, power plants, and process industries.

Circulating fluidized bed combustion (CFBC) technology holds great promise for power generation [2]. In CFBC, the flow enters the constant-diameter part of the cyclone tangentially and accelerates on its way down into the conical section, thereby resulting in a strong swirling flow with a complex flow pattern. At the base, the particle-laden flow escapes through the lower end, while the rest reverses and swirls along the centerline through the exit duct of the cyclone separator. The cyclone separator plays a major role in circulating fluidized bed boiler operation in power plants. A large number of solid materials are separated from the flue gas and then taken back to the furnace chamber, thereby establishing furnace material circulation [3]. This step can ensure that the fuel and the desulfurizer undergo a cycling combustion reaction

multiple times. Therefore, the circulating fluidized bed boiler has good combustion and desulfurization efficiency, and the circulating fluidized bed boiler can run on full load. The separation performance and operating status of a cyclone separator have a direct relationship with the combustion, desulfurization, and circulating rate of the circulating fluidized bed boiler [4]. A reliable computer design for predicting the effect of geometry changes and system parameters on cyclone efficiency would be a valuable tool. Such a design would help in optimizing the cyclone collector for specific operating conditions. A computational fluid dynamic (CFD) package with fluid flow equations that include turbulence losses can be applied to accomplish this task.

2. STATE OF THE ART

Numerous studies have focused on improving the performance of a cyclone and specifying the flow field behavior[5-9]. Azadi[10] investigated the effect of inlet velocity on the cyclone performance by using mathematical models. Gimbun [11] investigated the effect of cone tip diameter on cyclone performance through a CFD simulation and concluded that reducing the diameter increases the efficiency and pressure drop. Azadi [12] used a CFD model to study the effect of cyclone size on its performance. Their results indicated that the cyclone cut-off diameter and pressure drop increase as the cyclone size increases. Gao[13] investigated the effects of central channel parameters on the flow field in five cylindrical oil gas cyclone separators. Their results indicated that the diameter and height of central channel has an insignificant effect on the flow field in the separator chamber. They also analyzed the effects of decreasing and increasing the central channel diameter and height on pressure drop and tangential velocity.

Several turbulence models of the k-ɛ model, the RSM model, and a variation of the k-ɛ model were evaluated. Simulations were also compared with velocity measurements carried out through laser Doppler anemometry. The Reynolds stresses model exhibited the best behavior [14]. The large swirl velocity produces difficulties in computing viscous flow in the cyclone separator. Reynolds-averaged Navier–Stokes equation approaches with RSM are still widely used to predict velocity patterns and pressure drop across the cyclone separator [15]. To simulate the gas–solid flow in a cyclone, the RSM was used as a suitable turbulent model for strong swirling flow [16]. RSM forgoes the assumption of isotropic turbulence and solves a transport equation for each component of the Reynolds stress.

In recent years, experimental and theoretical investigations have been conducted to reduce the size and enhance the separation efficiency of the gas-solid cyclone separators. Su[17] simulated gas-solid flow in square cyclone separators with three inlet configurations. They analyzed the effect of inlet configurations on the turbulent dynamics in the cyclone and the separation efficiency and pressure drop. Their results showed that 3D RSM was suitable to predict the swirling suspension flow in the square separator. The separators with double declining inlets and single normal inlet had the minimum pressure drop and the best separation efficiency, respectively. Oh [18] predicted the internal flow field in a cyclone separator. Their results showed that the Eulerian-Lagrangian approach was adequate to simulate gas-solid mixture inside the cyclone. They concluded that a recirculation zone was present under the vortex finder and a helical flow in the carrier gas outlet.

Investigation of a full-size cyclone separator is seldom reported in existing literature. Exhaust pipe depth has a great effect on

flow conditions and performance of the cyclone separator during use in power plants. The problem of exhaust pipe deformation occurred during the application of the cyclone separator in power plants. This deformation has a direct relationship with the flow field distribution in cyclone separators. However, analysis of the effect of the exhaust pipe depth of cyclone separator is rare. Therefore, the effect of the exhaust pipe depth on the cyclone separator used for a 240 t/h circulating fluidized bed boiler of a power plant was investigated in this paper. The numerical simulation method is applied to simulate the flow field of a full-size cyclone separator to improve the operation and efficiency. The research results can provide guidance for industrial application of cyclone separator.

To understand the flow pattern in a cyclone separator, this paper presents an analysis in two aspects. The first part analyzes the velocity and pressure distribution inside the cyclone separator with modifications of exhaust duct used in power plant applications. The latter part presents the flow motion of particles inside the cyclone separator with modified exhaust ducts.

The remainder of this paper is organized as follows: Section 2 describes the cyclone separator and the numerical method. Section 3 presents the numerical simulation results. Conclusions are summarized in Section 4.

3. METHODOLOGY

3.1. COMPUTATIONAL DOMAIN AND DOMAIN DISCRETION

Figs. 1 and 2 show the site photo and the schematic of the cyclone separator, which is applied to a 240 t/h circulating fluidized bed boiler used in the manufacturing industry. The cyclone consists of an upper cylindrical part with a tangential inlet. These parts are used to separate dispersed heavy substance from a fluid of lower density. The suspension to be separated was injected with high velocity tangentially into the cyclone, thereby resulting in spin velocities within the cyclone. These high spin velocities produced a large centrifugal force field, thereby causing dense particles to drift toward the fluid. The separated material leaves the cyclone at its apex, while clean fluid is discharged at the top through the overflow pipe. The size of the cyclone separator is the same as the size used in industries without any simplification. The cyclone separator consists of an inlet segment, a straight cylinder segment, a conical barrel segment, an exhaust pipe, and an ash discharging pipe.

The exhaust pipe was deformed seriously during operation. This deformation resulted in performance degradation of equipment and necessitated design alternatives. Therefore, the effect of the exhaust pipe on the flow dynamics was analyzed in this paper.

FLUENT software was applied to study the flow dynamics of a cyclone separator used for a circulating fluidized bed. FLUENT software consists of preprocessing software GAMBIT and postprocessing software FLUENT. The establishment of a geometric model and the discrete grids of the computational domain were carried out in GAMBIT. The full-size geometric 3D model of the cyclone separator was accomplished in GAMBIT without any simplification. Fig. 3 shows the grid distribution of cyclone separator. The hexahedral grid was used in the entire calculation region according to the structure characteristics of the cyclone separator to improve the calculation accuracy and to control the grid number effectively. Mesh quality is an important factor concerning numerical simulations. Aiming the highest quality possible, only hexahedral elements were used in this work, i.e., avoiding the use of auto-



Fig. 1. Site photos of the cyclone separator used in CFBC plant

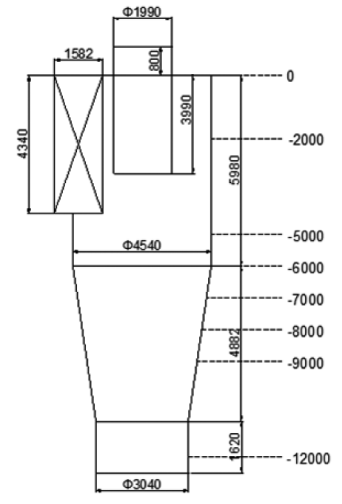


Fig. 2. Schematic diagram of cyclone structure

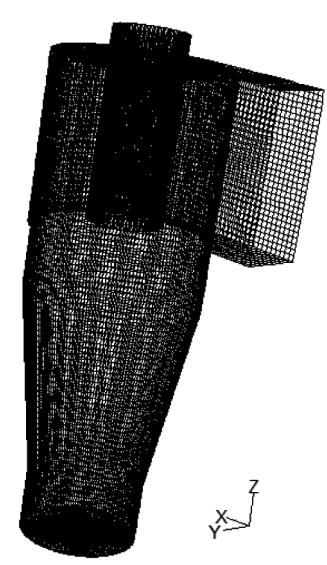


Fig. 3.Computational mesh for cyclone collector

matic generated meshes with quad dominant elements or tetrahedral elements, which may require a larger number of elements, due to numerical diffusivity. Although more laborious, this method allows, considering the simulation of this specific device, to obtain numerical grids with an overall higher quality. This, in turn, enables the use of fewer elements. In all CFD simulations, a mesh dependence test is crucial in order to check the convergence of the computational results with respect to spatial resolution. The effect of grid resolution on the inter-

$$u_{j}\frac{\partial u_{i}}{\partial x_{j}} = -\frac{\partial p}{\partial x_{i}} + \frac{\partial}{\partial x_{j}} \left(\mu \left(\frac{\partial u_{i}}{\partial x_{j}} + \frac{\partial u_{j}}{\partial x_{i}} \right) \right) + \frac{\partial \tau_{ij}}{\partial x_{i}}$$
(2)

where , and represent the time-averaged fluid velocity, pressure, density, and viscosity, respectively, and is the Reynolds stress. To solve the above equation, a turbulence model is needed to model the Reynolds stress tensor.

3.2.2. Turbulence model

The FLUENT code provides the k-ɛ, RSM, and other turbulent models for users to choose. RSM accounts for the evolutions of the individual stress components [14,19–20], thereby entirely avoiding the use of an eddy viscosity and is well suited for handling anisotropic turbulence fluctuations[17,21]. Therefore, this work applies RSM to simulate the gas flow in view of the flow condition in a cyclone separator. In the RSM, the transport equation is given as

$$\frac{\partial}{\partial t} \left(\rho \overrightarrow{u_i u_j} \right) + \frac{\partial}{\partial x_k} \left(\rho u_k \overrightarrow{u_i u_j} \right) = D_{ij} + P_{ij} + \phi_{ij} + \varepsilon_{ij} + S \tag{3}$$

where the two terms on the left-hand side of the above equation are the local time derivative of stress and convective transport term, respectively. The five terms on the right-hand side are the stress diffusion, the shear production, the pressure-strain, the dissipation, and the source term. The final transport equations of RSM can be written as follows:

$$\frac{\partial}{\partial x_{k}} \left(\rho u_{k} \overrightarrow{u_{i} u_{j}} \right) = \frac{\partial}{\partial x_{k}} \left[\frac{\mu_{i}}{\sigma_{k}} \left(\frac{\partial}{\partial x_{k}} \overrightarrow{u_{i} u_{j}} \right) \right] - \rho \left[\overrightarrow{u_{i} u_{k}} \frac{\partial u_{j}}{\partial x_{k}} + \overrightarrow{u_{j} u_{k}} \frac{\partial u_{i}}{\partial x_{k}} \right] + \overline{p \left(\frac{\partial u_{i}}{\partial x_{j}} + \frac{\partial u_{j}}{\partial x_{i}} \right)} - 2\mu \frac{\overline{\partial u_{i}} \frac{\partial u_{j}}{\partial x_{k}}}{\partial x_{k}}$$
(4)

ied by changing the cell numbers. For the current study, 320000 cells were used after considering the calculation economy with grid dependency and sensitivity. Calculation accuracy was verified by comparing the flow field in the cyclone separator. After completion of mesh generation with different parts, the assembled mesh imported in the flow solver is shown in Fig. 3.

nal flow field was stud-

3.2. SIMULATION MODEL AND BOUNDARY CONDITIONS

3.2.1. Governing equations

The gas flow in the cyclone was incompress-

ible because the Mach number was less than 0.3. For the steady and incompressible fluid flow in cyclones, the continuity equation for the mean flow and time-averaged Navier-Stokes equations for the gas flow were used.

$$\frac{\partial u_j}{\partial x_j} = 0 \tag{1}$$

 $[\partial x_k, \partial x_k] = [\partial x_j, \partial x_k] = [\partial x_j, \partial x_k] = [\partial x_k, \partial x_k]$ where the eddy viscosity, m_j is calculated by the following

$$\mu_{t} = \rho c_{\mu} \frac{k^{2}}{\varepsilon} \tag{5}$$

where C_{ii} is 0.09.

3.2.3. Gas-solid multiphase model

In this study, the Eulerian–Langrangian approach was used to calculate the trajectories of particles in the cyclone because the particle volume fraction was less than 10%[22]. In this case, the presence of the particles did not affect the flow field. The particle force balance equation in this case in x, y and z directions, respectively, can be written as

$$\frac{du_p}{dt} = F_D \left(u - u_p \right) + \frac{v_p^2}{r_0} \tag{6}$$

$$\frac{dv_p}{dt} = F_D \left(v - v_p \right) + \frac{u_p v_p}{r_0} \tag{7}$$

$$\frac{dw_p}{dt} = F_D \left(w - w_p \right) - g \tag{8}$$

where u_p , v_p , w_p are the velocity component of particles in the x, y, and z directions, respectively. v_p^2/r_o and $u_p v_p/r_o$ are the centrifugal and Coriolis components of particle acceleration, respectively. F_p is calculated by using the following equation:

$$F_D = \frac{18\mu_A}{\rho_p d_p^2} \frac{C_D \operatorname{Re}_p}{24} \tag{9}$$

$$C_D = C_1 + \frac{C_2}{\text{Re}_p} + \frac{C_3}{\text{Re}_p}$$
 (10)

$$\operatorname{Re}_{p} = \frac{\rho_{A} d_{p} \left| u_{p} - u_{A} \right|}{\mu_{A}} \tag{11}$$

where $\rho_{_A}$ is the air density, $d_{_P}$ is the particle diameter, and $\mu_{_A}$ is the dynamic viscosity of gas.

3.2.4. Selection of the discretization schemes and boundary conditions

Governing equations were solved numerically by the finite volume method using the commercial CFD code FLUENT 6.3.26. The semi-implicit method pressure-linked equations consistent algorithm was used for the pressure-velocity coupling. Pressure staggered option was used to interpolate the pressure because of highly swirling flows in cyclone. The Reynolds stress equations were solved based on the second-order upwind scheme discretization. In this study, these discretization schemes were used for all simulations.

The gas inlet boundary was set as the velocity boundary condition with a velocity of 15 m/s. The outflow boundary condition was applied for the outlet boundary. No slip boundary condition was adopted at the walls. The inlet velocity of particles was assumed the same as the gas inlet velocity. The gas turbulent flow was modeled by 3D RSM. The discrete phase model was used to calculate the particle trajectories in the gas flow. The accuracy of the CFD results is related to an adequate cell size with numerical models in a computational domain. The cell size should be sufficiently small to capture the effect of shear stress and velocity gradient on turbulent flow. The consideration of wall function is needed because turbulent flow is affected by the existence of a wall. The effect of the molecular viscosity on the flow plays an important role in the near-wall region, while the effect of turbulence on the flow has an important role in the fully turbulent region. Wall y+ was between 31 and 290. The size of the first cell is different in different region in cyclone separator. In the current study, the distance between the first cell center and the separator wall was calculated as $y^* = 0.83$ mm to consider the shear layer effect on an internal flow field of the cyclone separator. The pressure drop of the cyclone separator obtained from the numerical simulation agreed well with the pressure drop measured by experiment in power plant. Therefore, the simulation model proposed in this study is useful to predict the flow dynamics of the cyclone separator.

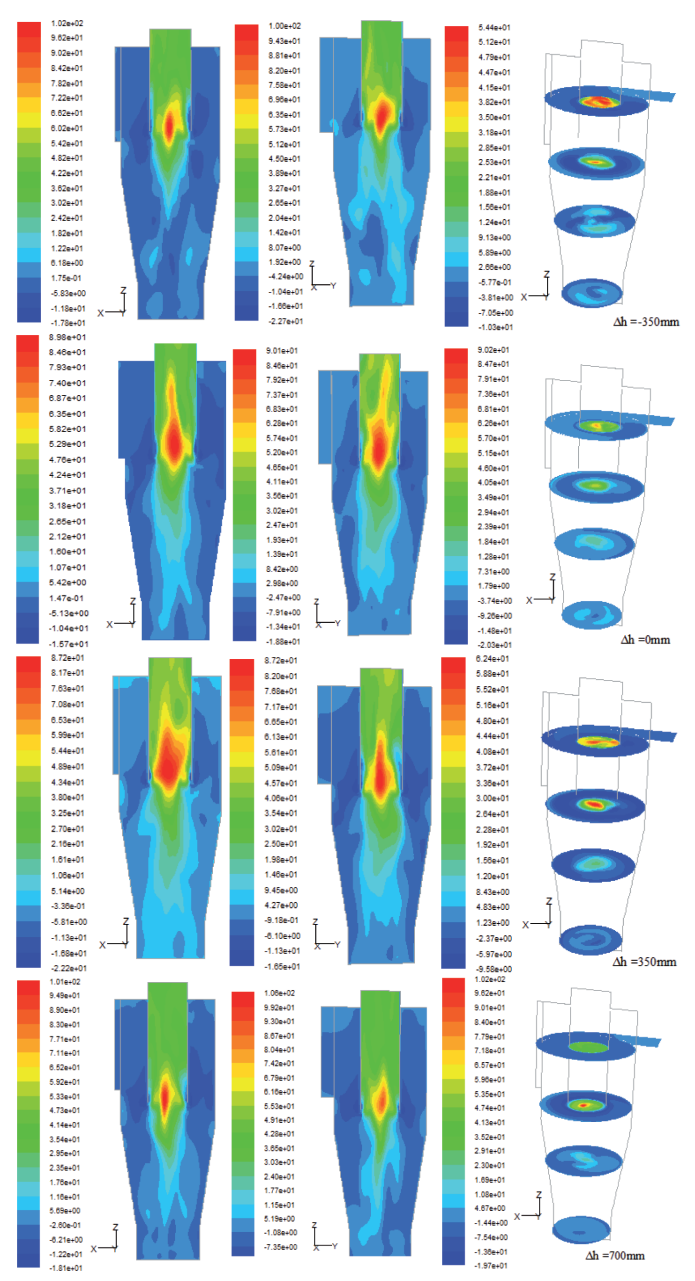
4.RESULT ANALYSIS AND DISCUSSION

Four cases of different depths of exhaust pipe were used to investigate the effect of the exhaust pipe on the flow dynamics in a cyclone separator. Simulations on the velocity distribution, pressure distribution, and particle trajectory under different insert depths h (h = 3990, 4340, 4690, and 5040 mm) were performed by using CFD technique. The relative depth Δh between the insert depth of the exhaust pipe and the height of the cyclone inlet was defined as Equation (12).

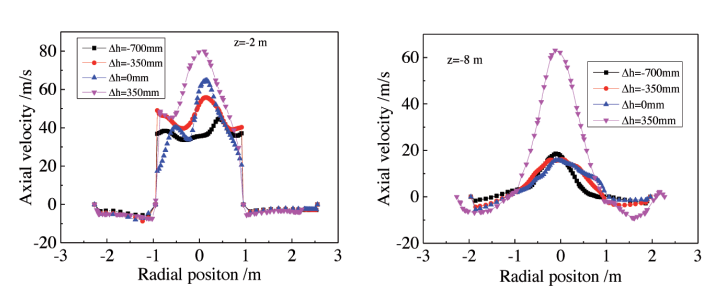
$$\Delta h = h - 4340 \tag{12}$$

Therefore, four cases of insert depth of the exhaust pipe were carried out; the relative insert depths of the exhaust pipe were Δh =-350mm, Δh =0mm, Δh =350mm and Δh =700mm. The minus

sign indicates that the insert depth of the exhaust is shorter than the height of the cyclone inlet. In case 1, the bottom of the exhaust pipe is 350 mm higher than the bottom of the inlet of the cyclone separator and 350 mm shorter than the inlet height of the cyclone separator. In case 2, the bottom of the exhaust pipe is at the same level as the bottom of the inlet of the cyclone separator. In case 3, the bottom of the exhaust pipe is 350 mm lower than the bottom of the inlet of the cyclone separator. In case 4, the bottom of the exhaust pipe is 700 mm lower than the bottom of the cyclone separator.



(a) Contour of axial velocity(m/s) at different sections



(b) Plot of axial velocity at different stations Fig. 4 The distribution of axial velocity of different insertion depth

4.1. VELOCITY DISTRIBUTION

Fig. 4 shows that the axial velocity varied with the insert depth of exhaust pipe at different positions. Fig.4 (a) shows the contour of axial velocity at different sections in cyclone separator. Fig.4 (b) presents the curves of axial velocity at different stations. The axial velocity distribution was essentially symmetrical in the straight cylinder and conical barrel segment. Gas flowed downwards near cyclone separator wall, while gas flowed upwards in the center of cyclone separator. The axial velocity increased in the exhaust pipe when the depth of the exhaust pipe decreased. The maximum value of axial velocity occurred in the case of Δh =350 mm. The axial velocity distribution at Δh =350 mm caused more small particles to escape from the exhaust pipe. The axial velocity was almost the same at the annular separation space. The maximum axial velocity did not occur at the center of the ash bucket. Therefore, no obvious particle retention occurred in this section.

Fig. 5 shows the radial velocity variation along the radial position at different heights. The radial velocity decreased with the increasing radius. The distribution trend of radial velocity changed minimally at different heights. An identical flow phenomenon was observed at the cyclone. The radial velocity profiles show that the

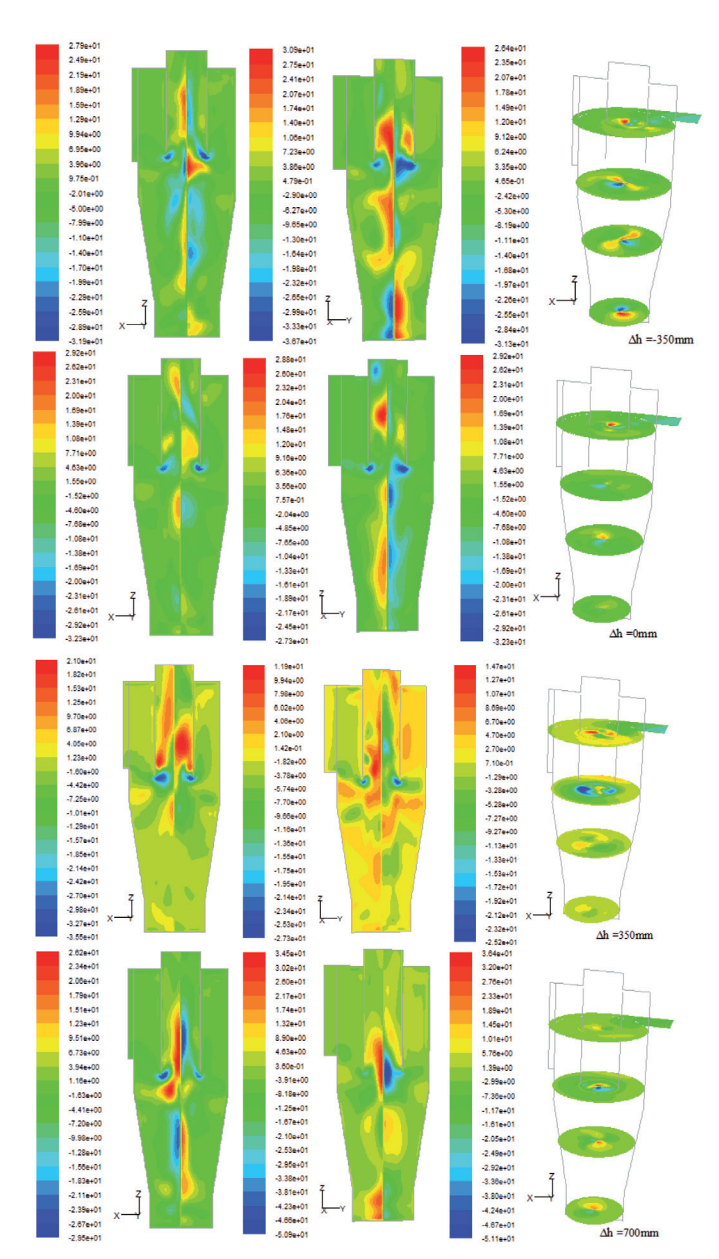
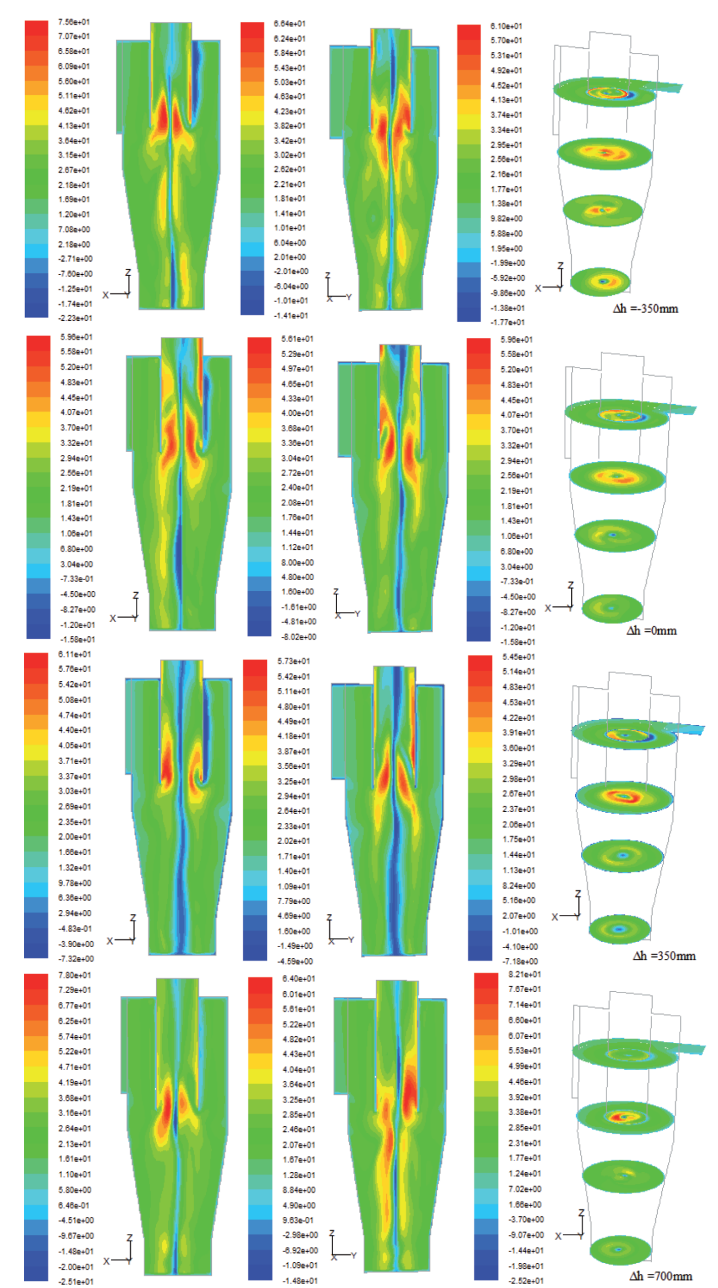


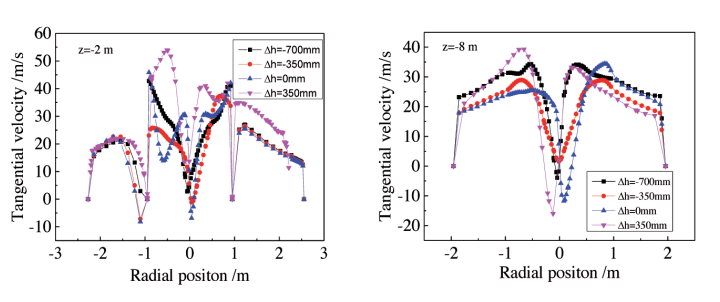
Fig. 5. The distribution of radial velocity (m/s) of different insert depth of exhaust pipe

flow in the cyclone separator was rotational and approximately symmetrical, thereby enhancing the transport of particles into the cyclone. The radial velocity was relatively high around the inlet of the exhaust pipe. Therefore, part of gas and small particles can enter the exhaust pipe and then leave the cyclone without the separating behavior of the cyclone separator.

Fig. 6 presents the tangential velocity at different positions for different exhaust pipe depths. The tangential velocity increased



(a) Contour of tangential velocity(m/s) at different sections



(b)Plot of tangential velocity at different stations Fig.6. The distribution of tangential velocity of different insert depth of exhaust pipe

with the increase of radius in the center of the cyclone separator. In this region, the fluid had the same angular velocity at different radial locations. The swirling flow in this region was called forced

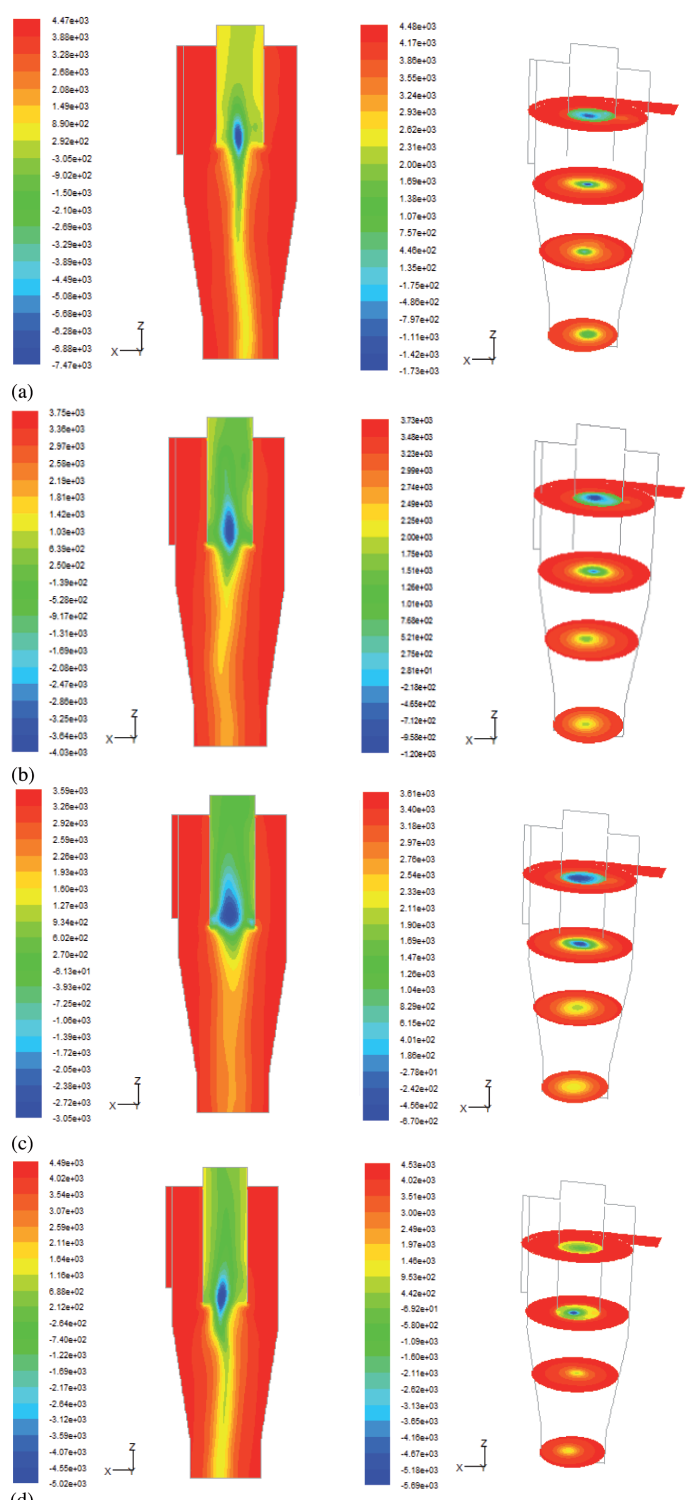


Fig. 7. Contours of relative static pressure (Pa) for Δh equals to: (a) Δh =-350mm, (b) Δh =0mm, (c) Δh =350mm and (d) Δh =700mm

vortex flow. The tangential velocity decreased with the increases of the radius at the region outside the center of the cyclone separator. In this region, fluid momentum is conserved, and the flow is described as free vortex flow. The insert depth of the exhaust pipe influenced the tangential velocity distribution more in the inlet segment and around the inlet of the exhaust pipe. Fig. 6(a) shows two more obvious vortexes than other three figures in the cyclone separator. One vortex is the outside vortex, which carries the gas and particles downward in the cyclone separator. The other vortex

is an inner upward vortex, in which the gas goes upwards. The two vortexes implement the separation process of particles from gas. Thus, the third case illustrates a better operation behavior among the four cyclone separators with different insert depths. The rotational velocity is larger in the center part of the separator when the insert depth of the exhaust pipe is shorter. The gas with larger rotational velocity may carry more particles leaving the separator. Therefore, the case 1 should be avoided, in which the insert depth Δh equals to $-350 \, \text{mm}$.

4.2. PRESSURE DISTRIBUTION

Fig. 7 shows the contours of relative static pressure in different depths of the exhaust pipe. A low pressure zone was observed in the center of the cyclones in all cases. The static pressure was higher near the cyclone separator wall than in the center of the cyclone separator. The internal swirl flow appeared in the center of the cyclone separator. Therefore, the lowest pressure occurred in this region. The static pressure distribution was essentially symmetric in the radial position. The deviation from the symmetric part was mainly due to the cyclone inlet airflow that entered the cyclone separator tangentially. The static pressure decreased from the ash discharging tube to the gas exhaust pipe entrance. As the depth of the exhaust pipe increased, this zone expanded first and then contracted. The pressure increased first and then decreased as the insert depth of the exhaust pipe increased. The maximum pressure drop occurred at the inlet of the exhaust pipe, which caused more gas and particles to flow into the exhaust pipe directly. Moreover, the force applied on the exhaust pipe increased as the pressure drop increased.

Fig. 8 presents the pressure variation with the depth of the exhaust pipe along the radial direction. The flow field was studied by analyzing the pressure distribution around the exhaust pipe inlet in the cyclone separator. z=-2 m is located in the circular region. The pressure in the center of the inlet segment decreased with the decrease of the depth of exhaust pipe. The pressure difference across the surface of the exhaust pipe was the largest at $\Delta h = -350$ mm. In this case, the exhaust pipe should suffer the largest pressure force.

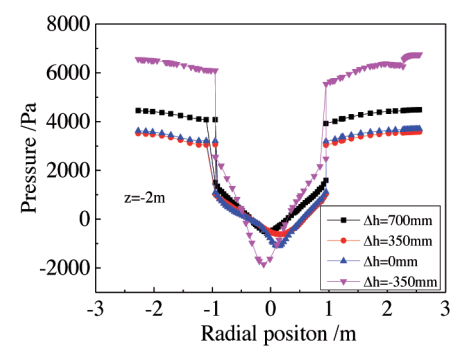


Fig. 8.The distribution of pressure at different insertion depth of exhaust pipe

4.3. PARTICLE FLOW INSIDE CYCLONE SEPARATOR

Particle trajectories of different size particles are shown in Figs. 9, 10, and 11. The particles were assumed to be collected when they touch the bottom wall surface of the cyclone separator. Fig. 9 illustrates that all the particles with a 5 μm diameter escaped from the cyclone separator in cases 1 and 2. Most particles with a 5 μm diameter escaped from the cyclone separator, with a small number of particles with a 5 μm diameter being collected in the cyclone separator in cases 3 and 4. Fig. 10 shows that more particles with a 30 μm diameter were collected when the insert

depth was longer than the inlet height of the cyclone separator. Fig. 11 shows the 50 μm diameter particle trajectories in different insert depths of the exhaust pipe. All the particles with a 50 μm diameter can be collected by the cyclone separator. Increasing the insert depth of the exhaust pipe can reduce the short circuit current around the exhaust pipe, thereby collecting more small particles. A long insert depth of the exhaust pipe corresponds to additional weight, which can lead to deformation of the exhaust pipe under the effect of gravity and pressure.

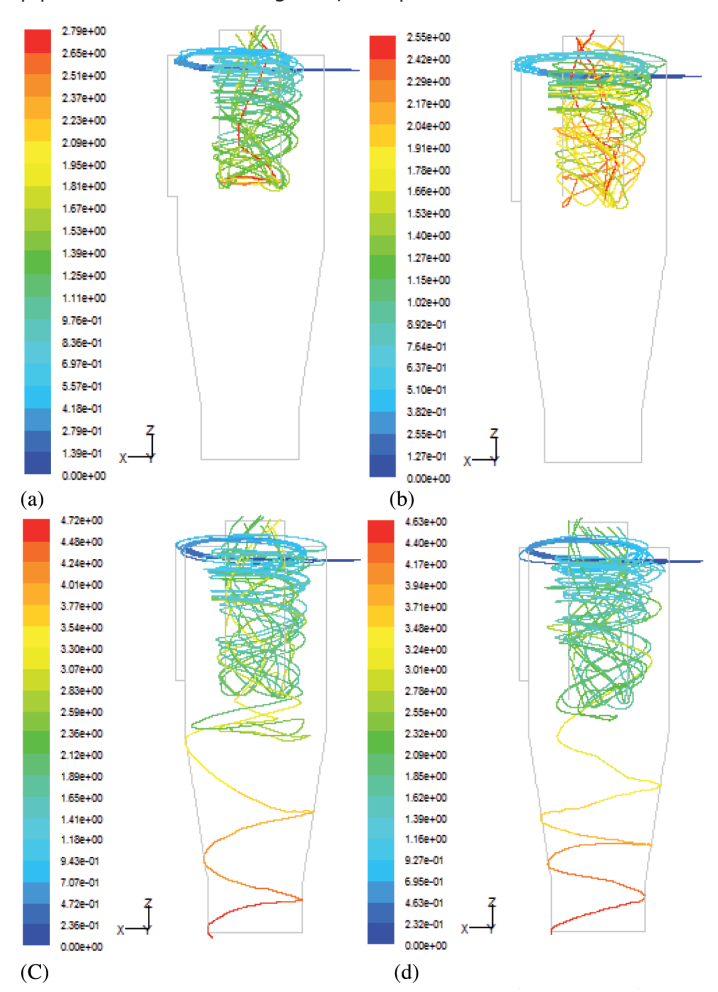


Fig. 9. The trajectories of particles with diameters of dp=5 μ m. (a) Δh =-350mm, (b) Δh =0mm, (c) Δh =350mm and (d) Δh =700mm

5. CONCLUSIONS

The RSM provided by FLUENT software was applied to study the flow field of a 3D and full-size cyclone separator used for a circulating fluidized bed. The stochastic Lagrangian model was used to predict the flow pattern of particles in the cyclone. The following conclusions can be drawn from this study:

The flow dynamic distribution is essentially symmetric in the cyclone separator. Gas flows downwards near the cyclone separator wall, while gas flows upwards in the center of the cyclone separator. The swirling flow in this center region is forced vortex flow.

The radial velocity is relatively high around the inlet of the exhaust pipe, which causes part of gas and small particles to enter the exhaust pipe and then exit the cyclone without being subjected to the separating behavior of cyclone separator.

The static pressure drop decreases first and then increases with increase of the insert depth of the exhaust pipe. The pressure drop is highest across the exhaust wall near the inlet of the exhaust pipe compared with other three insert depth cases. This pressure drop can generate a large force that acts on the exhaust pipe.

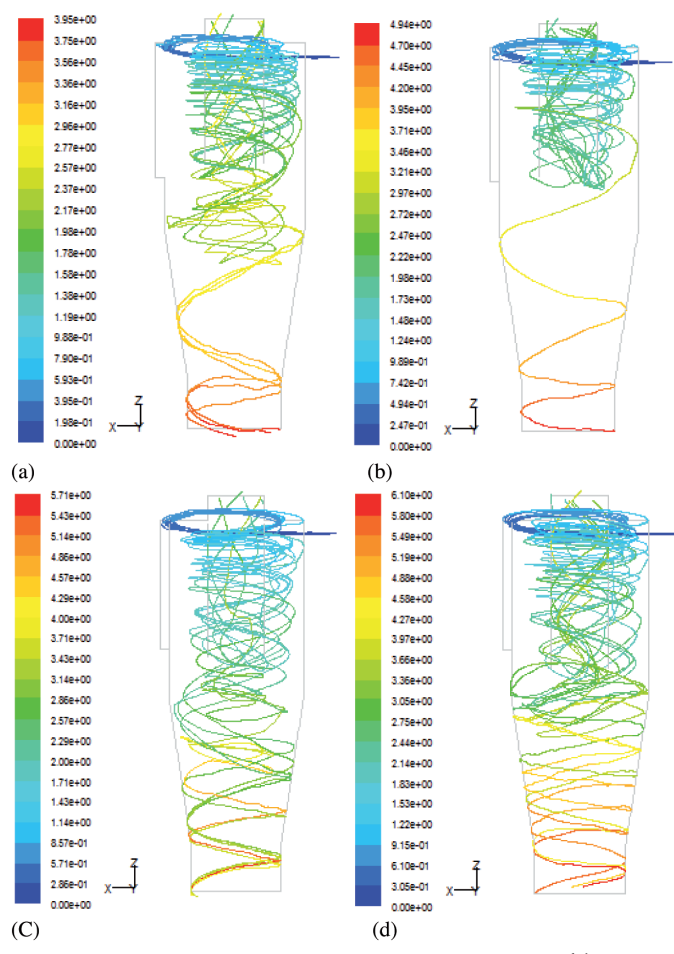


Fig. 10. The trajectories of particles with diameters of dp =30 μ m. (a) Δh =-350mm, (b) Δh =0mm, (c) Δh =350mm and (d) Δh =700mm

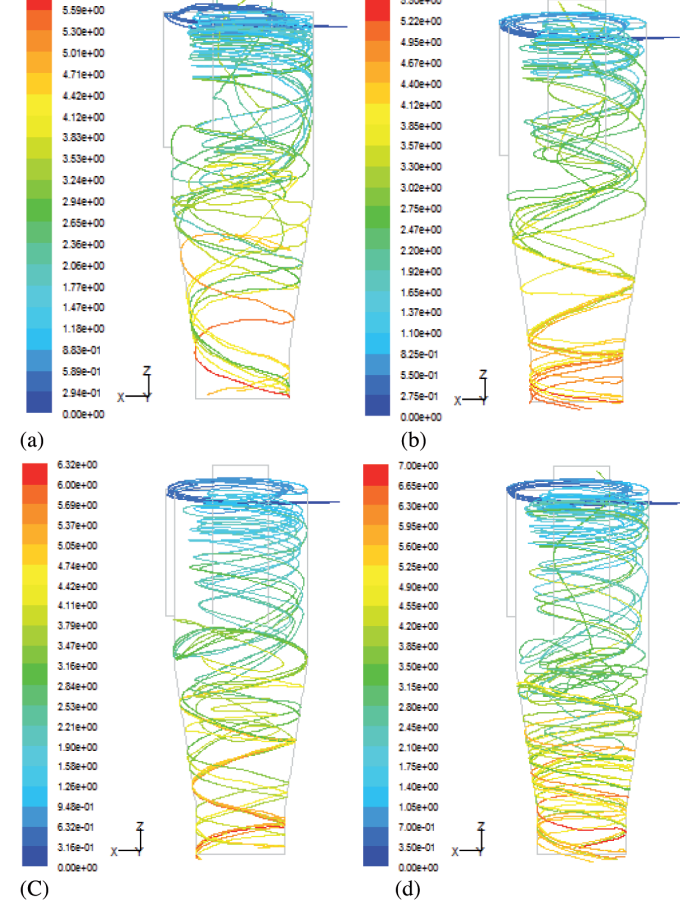


Fig. 11. The trajectories of particles with diameters of dp=50 μ m. (a) Δh =-350mm, (b) Δh =0mm, (c) Δh =350mm and (d) Δh =700mm

The number of particles that escape from the cyclone decreases when the insert depth of the exhaust pipe increases. Almost all particles whose diameter is larger than 50 μ m can be separated by the cyclone separators of four insert depths of the exhaust pipe. The particle separation efficiency is higher when the bottom of the exhaust pipe is lower than the inlet of the cyclone separator, such as in case 3 and case 4.

The results provide guidelines for cyclone separator design and operation, especially for improving the problem of exhaust pipe deformation. Nonetheless, this study suffers some limitations. Only one parameter of exhaust pipe insert depth was considered to investigate the operating behavior of the cyclone separator. Other parameters, such as the diameter of the exhaust pipe, also have an effect on operating behavior. The effect of exhaust shape on the force exerted on the exhaust pipe, the flow resistance in cyclone separator, the grade efficiency of particles should be taken into account in future extensions of this study.

BIBLIOGRAPHY

- [1] Khairy E, Chris L. Numerical modeling of the flow field and performance in cyclones of different cone-tip diameters. Computers and Fluids. January 2011. Vol.51-1.p.48-59. doi: http://dx.doi.org/10.1016/j.compfluid.2011.07.010
- [2] Bhasker C. Flow simulation in industrial cyclone separator. Advances in Engineering Software. February 2010.Vol.41–2. p. 220–228. doi: http://dx.doi. org/10.1016/j.advengsoft.2009.08.004
- [3] Zhao L. Center tube renewal analysis of 240 t/h circulating fluidized bed boiler. Plant Maintenance Engineering. August 2010.Vol.8-8. 41-42.doi: http://dx.doi.org/10.3969/j.issn.1001-0599.2010.08.023(in Chinese)
- [4] Hui S, Ji G, Jin Y, Wang J. Investigation on Separation Performance of Cyclone Separator Used in Circulating Fluidized Bed Boiler, China Powder Science and Technology, February 2008.Vol.14–2. p.42–44. doi: http://dx.doi.org/10.3969/j. issn.1008-5548.2008.02.013(in Chinese)
- [5] Oh J, Choi S, Kim J. Numerical simulation of an internal flow field in a uniflow cyclone separator. Powder Technology. April 2015.Vol.274-4. p.135-145. doi: http://dx.doi.org/10.1016/j.powtec.2015.01.015
- [6] Safikhani H, Akhavan-Behabadi M A, Shams M, Rahimyan M H. Numerical simulation of flow field in three types of standard cyclone separators. Advanced Powder Technology. April 2010.Vol.21-4. p.435-442. doi: http:// dx.doi.org/10.1016/j.apt.2010.01.002
- [7] Chen J, Liu X. Simulation of a modified cyclone separator with a novel exhaust. Separation and Purification Technology. February 2010. Vol.73-2. p.100-105. doi: http://dx.doi.org/10.1016/j.seppur.2010.03.007
- [8] Duan L, Wu X, Ji Z, Fang Q. Entropy generation analysis on cyclone separators with different exit pipe diameters and inlet dimensions. Chemical Engineering Science. September 2015. Vol.138-9. p.622-633. doi: http:// dx.doi.org/10.1016/j.ces.2015.09.003
- [9] Bhasker C, Flow simulation in industrial cyclone separator. Advances in Engineering Software. February 2010.Vol.41-1. p.220-228.doi: http://dx.doi.org/10.1016/j.advengsoft.2009.08.004
- [10] Azadi M, Azad, M. An analytical study of the effect of inlet velocity on the cyclone performance using mathematical models. Powder Technology. February 2012.Vol. 217-1.p.121-127. doi:10.1016/j.powtec.2011.10.017
- [11] Gimbun J, Chuah T G, Choong T S Y, et al. Prediction of the effects of cone tip diameter on the cyclone performance. Journal of Aerosol Science. August 2005.Vol.36-8. p.1056-1065. doi: http://dx.doi.org/10.1016/j. jaerosci.2004.10.014
- [12] Azadi M, Azadi M, Mohebbi A. A CFD study of the effect of cyclone size on its performance parameters. Journal of Hazardous Materials. March 2010. Vol.182-3. p. 835-841. doi: http://dx.doi.org/10.1016/j.jhazmat.2010.06.115
- [13] Gao X, Chen J, Feng J, Peng X. Numerical investigation of the effects of the central channel on the flow field in an oil-gas cyclone separator. Computer and Fluids. March 2014. Vol.92-3. p.45-55. doi: http://dx.doi.org/10.1016/j. compfluid.2013.11.001
- [14] Cristobal C, Antonia G. Modeling the gas and particle flow inside cyclone separators. Progress in Energy and Combustion Science. May 2007.Vol.33-5. p. 409-452. doi:10.1016/j.pecs.2007.02.001

- [15] Wang J, Mao Y, Liu M, Wang J. Numerical simulation of strongly swirling flow in cyclone separator by using an advanced rng k-emodel. Acta Petrolei Sinica (Petroleum Processing Section). January 2010.Vol.26-1. p.8-13. doi: http://dx.doi.org/10.3969/i.issn.1001-8719.2010.01.002(in Chinese)
- [16] Fathizadeh N, Mohebbi A, Soltaninejad S, et al. Design and simulation of high pressure cyclones for a gas city gate station using semi-empirical models. genetic algorithm and computational fluid dynamics. Journal of Natural Gas Science and Engineering. September 2015.Vol.26-9. p.313-329. doi:10.1016/j.jngse.2015.06.022
- [17] Souza F J, Vasconcelos R, Moro D. Effects of the gas outlet duct length and shape on the performance of cyclone separators. Separation and Purification Technology. March 2015. Vol.142-3. p.90-100. doi: http:// dx.doi.org/10.1016/j.seppur.2014.12.008
- [18] Su Y, Zheng A, Zhao B. Numerical simulation of effect of inlet configuration on square cyclone separator performance. Powder Technology. March 2011. Vol.210-3. p.293-303. doi: http://dx.doi.org/10.1016/j.powtec.2011.03.034
- [19] Liu S, Zhang Y, Wang B. Cyclone Separator Three-Dimensional Turbulent Flow-Field Simulation Using the Reynolds Stress Model. Journal of Beijing Institute of Technology. May 2005.Vol.25-5. p.377-380. doi: http://dx.doi.org/10.3969/j.issn.1001-0645.2005.05.001(in Chinese)
- [20] Mao y, Pang L, Wang X, Wu D. Numerical modeling of three dimension turbulent field in cyclone separator. Petroleum Processing and petrochemical. February 2002. Vol.32-2. p.32-37. doi: http://dx.doi.org/10.3969/j.issn.1005-2399.2002.02.001(in Chinese)
- [21] Safikhani H, Hajiloo A, Ranjbar M A.Modeling and multi-objective optimization of cyclone separators using CFD and genetic algorithms. Computers and Chemical Engineering. June 2011. Vol.35-6. p. 1064-1071. doi:http://dx.doi.org/10.1016/j.compchemeng.2010.07.017
- [22] Song J, Wei Y, Shi M. Asymmetry of gas-phase flow field in cyclone separator. Journal of Chemical Industry and Engineering. August 2005.Vol.56-8. p.55-60. doi: http://dx.doi.org/10.3321/j.issn:0438-1157.2005.08.004

APPRECIATION

This work was financially supported by the national natural science foundation of china (No. U1504217), Technological Major Special Project of Henan Province in China (No.508057), Scientific and technological project of Henan Province (102102210209) and Natural Science Foundation of Henan Province (2010B470005).